International Journal of Modern Manufacturing Technologies
ISSN 2067–3604, Vol. XIV, No. 1 / 2022
https://doi.org/10.54684/ijmmt.2022.14.1.55

OPTIMIZATION OF MAGNETIC ABRASIVE FINISHING PROCESS OF SS304 STAINLESS STEEL

Jagdeep Singh Gill[1], Lakhvir Singh[2]

[1]Mechanical Engineering Department, IKGPTU, Kapurthala, Punjab, India and Lecturer Baba Banda Singh Bahadur Polytechnic College, Fatehgarh Sahib (140407), Punjab, India
[2]Baba Banda Singh Bahadur Engineering College, Fatehgarh Sahib (140407), Punjab, India

Corresponding author: Jagdeep Singh Gill, erjsgill@gmail.com

Abstract: With the advancement of the high-end industry, the demand for smooth surfaces has grown at an exorbitant rate. Magnetic abrasive finishing (MAF) is gaining wide attention these days as a popular finishing method to achieve smooth and high-quality surfaces. An alternative approach was used in the present work to produce a highly finished surface on stainless steel SS304 sheet using a magnetic abrasive finishing process. Response surface methodology (RSM) was applied to optimize the process parameters. Optimal results occur at a magnetic flux density (3100 Gauss), the rotational speed of the magnetic pole (250 rpm), grit size (250µm), and the percentage of abrasive particles (10%) for a percentage reduction in surface roughness (%∇Ra). Among the four factors, the grit size of the abrasives is the factor with the highest contribution (42.70%) and the rotation speed of the magnetic pole is the factor with the least contribution (0.79%) during the finishing process of the magnetic abrasive, which affects the percentage reduction in surface roughness (%∇Ra). To acquire a better understanding of the finishing mechanism, scanning electron microscope (SEM) images and surface profiles of the surface before and after magnetic abrasive finishing were also examined.

Key words: Magnetic abrasive finishing (MAF), magnetic flux density, Design of experiments, Sintering, Response Surface Method (RSM), SEM, ANOVA.

1. INTRODUCTION

With the advancement in the high-end industry, the demand for smooth surfaces has grown at an exorbitant rate. Industries are adopting many new finishing methods to meet the demands for smooth and quality surfaces as traditional techniques (like grinding, polishing, buffing and lapping etc.) fail to meet the requirements or production cost increases due to these demands. Magnetic abrasive finishing (MAF) is one of the advanced finishing methods, used widely to obtain ultra-fine surfaces. Using a flexible tool composed of magnetized abrasive particles, the workpiece is finished in this process. The choice of the abrasive used depends upon the material to be worked on and its hardness. It achieves surfaces with nanometer-level roughness both on flat surfaces and on cylindrical surfaces, both internally and externally. In addition, non-rotatable workpieces such as bent tubes and elbows can be finished using this method.

Several researchers have studied the MAF process. As part of their study on finishing characteristics in magnetic abrasive processes, Shinmura et al. (1984) investigated how various working factors affected finishing characteristics. They stated that vibrating a workpiece boost finishing efficiency, stock removal, and reduces surface roughness. Jain et al. (2001) studied the effect of workpiece circumference speed and the working gap on the performance of the magnetic abrasive finishing process. They concluded based on their results that decreasing the circumferential speed and increasing the gap in the workpiece, respectively, decreases the amount of material removed. For finishing an anti-friction bearing steel workpiece (AISI 52100) having a hardness value of 61HRC, Mulik and Pandey (2010) developed and built an advanced MAF set up by using an electromagnet with alternate north and south poles. Based on experimental data, mesh number is the most significant predictor of surface roughness change, followed by percentage weight of abrasives, rpm of electromagnets, and voltage. With 70V electromagnet supply voltage, 280rpm rotation, 800 mesh SiC mesh sizes, and 15% abrasive, they were able to achieve surface roughness of 51nm within 120s of processing time. Riveros et al. (2013) examined the geometry and texture of nanoscale surface features to study the finishing characteristic of the MAF process of silicon flat chips. After experimenting, they concluded that the MAF process improved the surface roughness of features with little disruption to their overall geometry. Verma et al. (2016) developed a MAF-based novel tool for polishing holes and grooves. A central composite design (CCD) analysis was used to evaluate the performance of the tool developed and to determine the effects of parameters such as rotation speed, magnetic flux density, abrasive size, and abrasive weight percentage on the PISF of stainless-steel pipe (SS304). According to them, magnetic flux density was the most important parameter, followed by rotational speed, when finishing the SS304 pipe. Jain et al. (2016) investigated the effects of process parameters on the finishing forces generated during vertical magnetic abrasive finishing of ferromagnetic (EN-8) and non-ferromagnetic (Brass) flat workpieces. They concluded that more current supplied and a smaller working gap resulted in an increase in normal force and tangential force during magnetic abrasive finishing. Amnieh et al. (2017) developed a frustum-shaped polishing tool that is attached to a CNC machine to follow the polishing procedure on samples with a complex shape profile. In their experiment, they found that both the rotational speed of the magnetic tool and the finishing time-correlated directly with the surface roughness. Kajal et al. (2017) finished the barrel of a 0.32 in. revolver using MAF. During their experiments, they found that a rifled barrel is less likely to be finished than an unrifled barrel, and the value of the finishing rate decreased as rotational speed increased. A study by Wang et al. (2017) examined the Magnetic Abrasive Finishing of the inner surface of Al 6063 pipe, which is used in electronics, navigation, communications, among other things. Their report indicated that using the magnetic abrasive finishing method, the inner surface of the Al 6063 pipe had been successfully finished. Kumar et al. (2019) investigated the influence of four input process parameters (current, amount of magnetic abrasive, rotational speed, and percentage of the diamond abrasives) on percentage improvement in surface finish (PISF) and material removal rate (MRR). In experiments designed using the response surface method, they found that magnetic abrasives have a greater impact on PISF than rotational speed. Xie and Wu (2019) studied the magnetic abrasive finishing process for 5052 aluminum alloy plates. They reported that the finishing force increased with an increase in the particle size and that the magnetic field frequency had little effect on the maximum value of the finishing force. Yin et al. (2019) improved the dimensional accuracy of AISI 304 bars by using ultra-high-speed magnetic abrasive machining. Surface roughness improved from 0.32 µm to 0.03 µm in 40 seconds with the best performance at 80000 rpm. By using a magnetic abrasive finishing process, Li et al. (2020) studied the effect of a tapered magnetic head on the processing of titanium alloy wire. Simulating magnetic induction in the processing area with Maxwell software led to finding that magnetic heads with 0º taper have the lowest intensity whereas magnetic heads with 37º taper have the highest magnetic induction intensity. They achieved 0.28 µm of surface roughness in 300 s using a 37º taper magnetic head. Nam et al. (2020) finished beta-titanium wire using multiple transfer movements. In their study, 2000 rpm, particle size of 1 mm, and processing time of 300 seconds led to the best surface roughness Ra. Beta-titanium's surface roughness improved from 0.32 µm to 0.05 µm. To improve the flatness of plane surfaces, Zhang and Zou (2021) proposed using a variable speed magnetic abrasive finishing method. They controlled the machining duration over the surface of the workpiece by varying the speed of the finishing tool. On an A5052 aluminum alloy plate, they managed to reduce the extreme difference in the surface roughness from 14.317 µm to 2.18 µm, as well as the standard deviation from 3.222 µm to 0.417 µm. Lee and Chang (2021) used horizontal transverse magnetic fields for finishing aluminum specimens. In their experiments, they found that green silicon carbide achieves better results than white alumina for aluminum specimens. During the magnetic abrasive finishing process, Xie and Zou (2021) studied the effect of changing the mode of current on the magnetic flux and finishing force. As a result of experimentation, they discovered that pulse current produces a greater material removal rate than static magnetic field or sinusoidal alternating magnetic field. Ahmadi et al. (2021) performed full factorial analysis to evaluate the effects of particle morphology, workpiece material, machining time, speed of finishing, and specific abrasive powder used in the magnetic abrasive process. In their experiments, they found that rod-shaped abrasive particles performed much better than spherical ones on surface finish.

The literature survey shows that magnetic abrasive finishing is gaining wide attention these days as a popular finishing method to achieve smooth and high-quality surfaces. An alternative approach was used in the present work to produce a highly finished surface on stainless steel SS304 sheet using a magnetic abrasive finishing process. The abrasive particles were placed over the surface of the workpiece instead of being in direct contact with the magnetic pole as found in earlier studies. The machining tool (abrasives) will now be more flexible during finishing as a result of this procedure. Experiments were designed to evaluate the effect of process parameters on the response variable. Response surface methodology was applied to develop a model and to optimize the process parameters. The process parameters selected are magnetic flux density, the rotational speed of the magnet, the particle size of magnetic abrasives, and the percentage of abrasive particles in magnetic abrasives. The percentage reduction in surface roughness (%∇Ra) of the stainless steel SS304 sheet has been considered as the response variable. To acquire a better understanding of the finishing mechanism, scanning electron microscope (SEM) images and surface profiles of the surface before and after magnetic abrasive finishing were also examined.

2. MATERIALS AND METHODS

2.1 Experimental setup

In this study, a rotating magnetic pole system is used for finishing plane workpieces with magnetic abrasives. The experimental setup consists of a magnetic chuck, a worktable, and a direct current (D.C.) motor with a variable D.C. supply. A plane workpiece made of SS 304 stainless steel sheet (200 x 200 x 2 mm) is mounted on the worktable. Sintered magnetic abrasives were placed on the surface of the plane workpiece. “Magnetic abrasive particles (MAPS)” introduced over the workpiece are joined together. This yields a “flexible magnet abrasive brush (FMAB)” that pushes hard against the surface of the workpiece to develop finishing pressure. A magnetic pole fixed in a magnetic chuck is given rotary motion while the workpiece clamped over the table remains stationary during the finishing operation. A workpiece's surface is finished by the FMAB's relative motion to the workpiece.The change of distance between the magnetic chuck and the table on which the workpiece is clamped enables varying the magnetic field strength and thus the cutting force during experimentation.

2.2 Magnetic abrasives

This study used diamond-based sintered magnetic abrasives to finish plane workpieces made of SS 304 stainless steel. Various percents of iron powder, with a mesh size of 300, and diamond powder, with a mesh size of 250, were mixed to form diamond-based sintered magnetic abrasives. The powder mixture was compacted using a “universal testing machine (UTM)”, and then the compacts were sintered at 1100°C in an H_2 environment for 2 hours. Sintered compacts are ground into small particles and then sieved into sizes based on their size range. A sieve set was used to segregate abrasive particles. Different sieves having a size of 45, 75, 125, 200, 300, and 600 microns were used for this purpose. The different grit sizes of magnetic abrasives obtained were (+45/-75) 60μm, (+75/-125) 100μm, (+125/-200) 163μm, (+200/-300) 250μm, (+300/-600) 450μm. Figure 1 shows a photograph of the die used to prepare compacts. Following the sintering process, Figure 2 shows a photograph of the cylindrical compacts. The Diamond and iron particles were cohered during the sintering process and behaved as a single entity when the sintered powder was used during the magnetic abrasive finishing.

2.3 Response surface methodology

The response surface methodology is primarily used in situations where several input variables may affect a performance measure of a product. This performance measure is called response. The method consists of independent variables that are used to determine the outcome of the experiment. Box and Hunter developed a method known as central composite design, which fits second-order response surfaces. So, in the present study, the experiment was designed based on “Response Surface Methodology (RSM)” using “Central Composite Design (CCD)”. The level and number of process parameters were selected on the basis of the literature studied and the capability of the developed setup. In the current CCD, 4 independent factors at 5 different levels for experimentation have been chosen. This design generates 30 trail runs. Therefore, 30 random experiments were performed to finish the experiment.

Fig. 1. Photograph of the die used to prepare compacts

Fig. 2. Photograph of the cylindrical compacts

2.4 Surface roughness measurement

Table 1 shows the experimental conditions, while Table 2 shows the levels of input variables. Grit size, the percentage of abrasives, rotational speed, and magnetic flux density were used as input variables in the experiments. Machining time, amount of lubricant and quantity of abrasives were taken as constant parameters after conducting some preliminary experiments. Using "Mitutoyo's surface roughness tester (SJ-210P)" with a least count of 0.001 µm (cut-off length = 0.8 mm), the arithmetic average (R_a) surface roughness of the workpiece was calculated at four points before and after finishing. The final value of roughness is taken as the average of four readings. For obtaining a uniform value of initial roughness, an abrasive paper was used to roughen samples before magnetic abrasive finishing. A sample's roughness initial value R_a ranged from 0.984 µm to 1.112 µm. Experiments were conducted as per experimental design. As small cutting forces are involved in this process, a machining time of 2 hours is selected for doing experimentation.A percentage reduction in surface roughness (%∇Ra) was taken into account when evaluating the process. To calculate the percentage reduction in the surface roughness (%∇Ra), the following is the formula:

$$\%\nabla Ra = \frac{(Initial\ roughness - Final\ roughness) * 100}{Initial\ roughness} \quad (1)$$

Table 1. Experimental Conditions

Workpiece Material	SS 304 Stainless steel sheet (200x 200 x 2mm)
Machining Time	2 Hrs
Lubricant	Light Oil(5% of the quantity of abrasives)
Type of the abrasives	Diamond based sintered magnetic abrasives
Weight of Magnetic abrasives used	20g
Permanent magnet (2)	Magnet material Nb-Fe-B (50x50x50mm)
Response	%∇Ra (%)

3. RESULTS AND DISCUSSION

The major goal of this experiment was to examine the impact of various magnetic abrasive finishing parameters on the surface finish of a commercially available sheet of SS 304 stainless steel. Table 3 summarizes the results of the experiments.The experiment results using DESIGN EXPERT 8 software were analyzed.

Table 4 indicates that the model is crucial because the Model F value is 30.69.The likelihood of a "Model F-value" of this size due to noise is less than 0.01%. Model terms will be significant if probabilities > F are less than 0.0500.Here, A, C, D, AB, AD, CD, A^2, B^2, C^2, D^2 are significant model terms. The model terms are considered insignificant when their values exceed 0.1000. The "Lack of Fit F-value" of 4.60 implies there is a 5.29% chance that a "Lack of Fit F-value" this large could occur due to noise. The measure of the signal-to-noise ratio is "Adequacy Precision.". "Pred R-Squared" of 0.8200 is reasonably in agreement with the "Adj R-Squared" of 0.9348.A ratio greater than 4 indicates an adequate signal and in our case, the ratio is 19.028.You can use this model to explore the design area. The contribution of each factor is magnetic flux density (30.7 %), the rotational speed of the magnet (0.79 %), grit size (42.70 %), and the percentage of abrasive particles (1.53%) for a percent reduction in surface roughness (%∇Ra).

Table 2. Level of input variables for experimentation

Input Process Parameter	"Coded Parameter"	Level 1	Level 2	Level 3	Level 4	Level 5
Magnetic Flux Density (Gauss)	A	2800	2900	3000	3100	3200
Rotational Speed (rpm)	B	200	250	300	350	400
Magnetic Abrasive Particles Size (µm)	C	(+45/ -75) 60	(+75/ -125) 100	(+125/ -200) 163	(+200/ -300) 250	(+300/ -600) 450
Percentage of Abrasive (%)	D	5	10	15	20	25

"Response Surface Methodology (RSM)" was used to examine the effects of different process parameters on the percent reduction in surface roughness (%∇Ra) based on factors such as rotational speed of the poles, abrasive grit size, percentage of abrasives, and magnetic flux density (MFD). Removing the insignificant factors, the equation representing the model is:

$$\%\nabla Ra = +75.28333 + 11.12000 \times \text{Magnetic Flux} + 3.07750 \times \text{Size} - 2.47167 \times \text{abrasive percentage} - 3.83750 \times \text{Magnetic Flux} \times \text{Speed} + 4.13625 \times \text{Magnetic Flux} \times \text{abrasive percentage} - 3.30500 \times \text{Size} \times \text{abrasive percentage} - 5.54062 \times (\text{Magnetic Flux})^2 - 3.94063 \times (\text{Speed})^2 - 3.78062 \times (\text{Size})^2 - 4.23937 \times (\text{abrasive percentage})^2$$

Table 3. Result of experiments

Run	A: MFD (Gauss)	B: Speed (rpm)	C: Size (µm)	D: Abrasive Percentage (%)	Initial roughness (µm)	Final roughness (µm)	Response-%∇Ra (%)
1	2900	350	100	20	1.042	0.706	32.2
2	3000	300	163	25	0.986	0.488	50.5
3	3000	300	163	15	0.986	0.223	77.4
4	3000	200	163	15	1.108	0.537	51.5
5	2900	250	250	20	1.084	0.475	56.2
6	3000	300	163	15	1.102	0.260	76.4
7	2900	350	100	10	0.998	0.549	45.0
8	2900	350	250	10	0.992	0.170	82.8
9	3100	250	100	20	0.988	0.369	62.6
10	3000	300	163	15	1.028	0.244	76.2
11	2800	300	163	15	1.106	0.807	27.0
12	3100	350	100	20	1.024	0.362	64.6
13	2900	250	100	20	1.028	0.779	24.2
14	3100	250	250	10	1.064	0.124	88.3
15	2900	250	100	10	1.104	0.802	27.3
16	3200	300	163	15	1.024	0.272	73.4
17	3000	300	163	5	1.112	0.441	60.3
18	3000	300	450	15	1.01	0.209	79.3
19	3100	250	250	20	0.984	0.171	82.6
20	3100	350	250	20	0.992	0.227	77.1
21	3000	300	60	15	1.088	0.705	35.2
22	2900	350	250	20	1.044	0.478	54.2
23	3100	250	100	10	1.012	0.439	56.5
24	3000	300	163	15	0.986	0.238	75.8
25	2900	250	250	10	0.99	0.349	64.7
26	3100	350	100	10	0.996	0.515	48.2
27	3100	350	250	10	1.048	0.204	80.5
28	3000	300	163	15	1.11	0.331	70.2
29	3000	300	163	15	1.064	0.261	75.4
30	3000	400	163	15	1.076	0.411	61.7

3D graphs were generated to assess the impact of selected input parameters on the response (%∇Ra).

3.1 Effect of MFD (A) and Rotational Speed (B) on the %∇Ra

Figure 3 illustrates that initially,%∇Ra increases by increasing the magnetic flux density and rotational speed of the poles. But for the maximum rotational speed of the poles (400 rpm),%∇Ra starts to decrease when the magnetic flux density is increased above 3100 Gauss.%∇Ra keeps on increasing with an increase in magnetic flux at minimum value of the rotational speed of the poles (200 rpm). Maximum %∇Ra is obtained at an intermediate value of rotational speed (300rpm) and a maximum value of magnetic flux (3200 Gauss). It is observed that at a low value of the magnetic flux, by increasing the rotation speed of the magnetic poles, the material removal by abrasives per unit time increases, resulting in smoother surfaces. With a higher value of magnetic flux, with increasing speed, the abrasive particles begin to leave the working area, which leads to a decrease in the value of the change in roughness. The same phenomenon was reported by Singh et al. (2004).

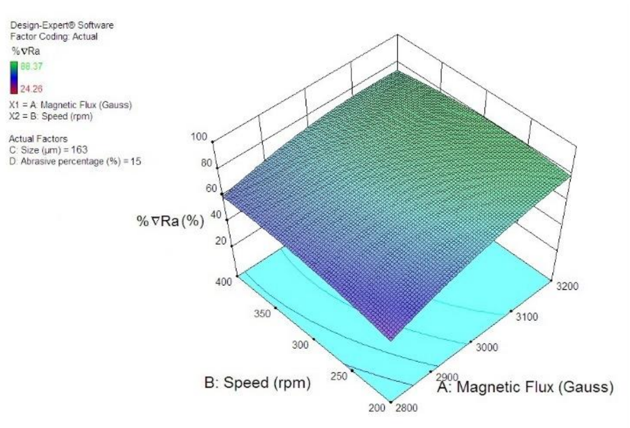

Fig. 3. Interaction effects of MFD (A) and Rotational Speed (B) on the %∇Ra

3.2 Effect of Grit size of abrasive (C) and MFD (A) on the %∇Ra

In Figure 4, the interaction between the magnetic flux density and the grit size of magnetic abrasives on %∇Ra is shown. %∇Ra starts to increase with an increase in the magnetic flux density and the grit size of the magnetic abrasives. Maximum %∇Ra is obtained at the maximum value of magnetic flux density (3200 Gauss) and the maximum grit size of magnetic abrasives (450 µm). This is due to the fact that as the magnetic flux density and size of magnetic abrasives are increased, more force acts on the surface. This removes the surface irregularities and higher %∇Ra is obtained. The same phenomenon was previously reported by Girma et al. (2006), in which they found that increased MAP grain size is beneficial to achieving a good surface finish.

Table 4. ANOVA Table

“ANOVA for Response Surface Quadratic Model”							
Source	**“Sum of Squares”**	**df**	**“Mean Square”**	**“F-Value”**	**“P-value”**	**Percentage contribution (%)**	
Model	9612.115	14	686.5796	30.689	< 0.0001		Significant
A-Magnetic Flux	2967.706	1	2967.706	132.6516	< 0.0001	30.87	
B-Speed	75.89927	1	75.89927	3.392575	0.0853	0.79	
C-Size	4104.504	1	4104.504	183.4647	< 0.0001	42.70	
D-%age	146.6193	1	146.6193	6.553644	0.0218	1.53	
AB	235.6225	1	235.6225	10.53194	0.0054	2.45	
AC	66.34103	1	66.34103	2.965337	0.1056	0.69	
AD	273.737	1	273.737	12.2356	0.0032	2.85	
BC	16.85103	1	16.85103	0.753214	0.3991	0.18	
BD	18.44702	1	18.44702	0.824552	0.3782	0.19	
CD	174.7684	1	174.7684	7.811865	0.0136	1.82	
A^2	842.0167	1	842.0167	37.63678	< 0.0001	8.76	
B^2	425.9253	1	425.9253	19.03817	0.0006	4.43	
C^2	392.04	1	392.04	17.52355	0.0008	4.08	
D^2	492.9545	1	492.9545	22.03427	0.0003	5.13	
Residual	335.5826	15	22.37217				
Lack of Fit	302.6935	10	30.26935	4.601725	0.0529		Not Significant
Pure Error	32.88913	5	6.577827				
Cor Total	9947.697	29					
Std. Dev.	4.729923243	“R-Squared”			0.966265297		
Mean	61.28233333	“Adj R-Squared”			0.934779574		
C.V. %	7.718249267	“Pred R-Squared”			0.81997092		
PRESS	1790.874768	“Adeq Precision”			19.02753569		

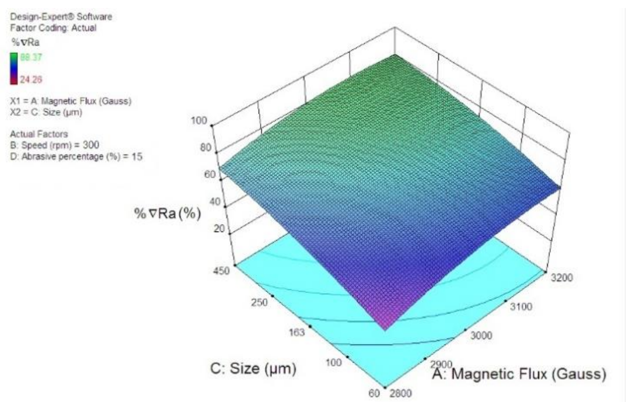

Fig. 4. Interaction effects of MFD (A) and Grit size of abrasive (C) on the %∇Ra

3.3 Effect of MFD (A) and %age of abrasives (D) on the %∇Ra

Keeping rotational speed and grit size of abrasive constant at intermediate value, Figure 5 illustrates the interaction effect of Magnetic Flux Density and percentage of diamond in magnetic abrasives on %∇Ra. %∇Ra increases as magnetic flux increases for a particular percentage of diamond in magnetic abrasives. Maximum %∇Ra is obtained at a higher value of magnetic flux density (3200 Gauss) and an intermediate value of diamond percentage (15%).

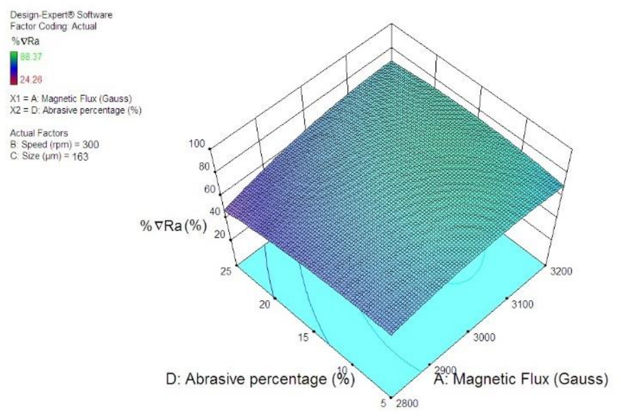

Fig. 5. Interaction effects of MFD (A) and %age of the abrasive (D) on the %∇Ra

%∇Ra decreases in small increments as the percentage of diamond in magnetic abrasives increases at lower values of MFD. As the percentage of diamond in abrasives increases, the %∇Ra does not differ significantly at higher MFD values. The increase in magnetic flux increases the strength and density of the tool. As previously reported by Singh et al. (2005), this results in a larger cutting force acting on the surface and a larger change in surface roughness value.

3.4 Effect of rotational speed (B) and Size of abrasive (C) on the %∇Ra

Figure 6 displays the effect of the rotational speed of the poles and grit size of the abrasive on %∇Ra, keeping the magnetic flux density and diamond percentage in magnetic abrasives constant at intermediate value. %∇Ra increases with an increase in the size of the abrasive at a particular value of the rotational speed of the poles. %∇Ra is less at a lower value of rotational speed (200 rpm) and smaller grit size of magnetic abrasives (60 µm). Less abrasion takes place at low speed and with a small abrasive grit size, which results in a lower value of %∇Ra. As rotational speed increases, the variation in %∇Ra for a particular grit size is not significant.

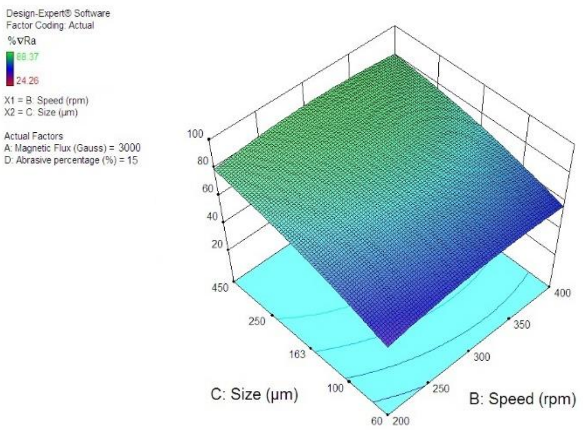

Fig. 6. Interaction effects of Rotational Speed (B) and grit size of abrasive (C) on the %∇Ra

3.5 Effect of rotational speed (B) and %age of abrasive (D) on the %∇Ra

In Figure 7, speed of rotation and diamond percentage in magnetic abrasives are considered to be the interaction parameters with regard to %∇Ra, while MFD and grit size are kept constant at intermediate value. At higher rotational speeds (400 rpm), %∇Ra decreases as diamond content increases from 5% to 25%, but at lower value of speed (200 rpm), %∇Ra varies insignificantly as abrasive content increases. The %∇Ra changes very little with increasing rotational speed at low diamond content(5%) in magnetic abrasives. The %∇Ra decreases slightly with increasing rotational speed from 200 to 400 rpm at maximum value of the percentage of abrasives (25%).

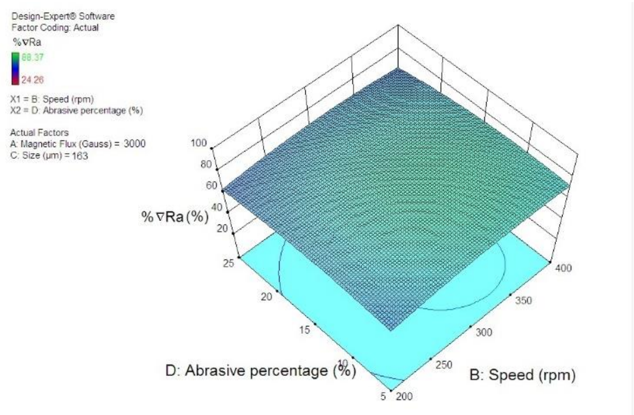

Fig. 7. Interaction effects of Rotational Speed (B) and %age of the abrasive (D) on the %∇Ra

3.6 Effect of grit size (C) and % age of the abrasive (D) on the %∇Ra

Figure 8 plots the interactions between the abrasive grit size and the diamond content in the magnetic abrasives on %∇Ra while keeping both the rotational speed and MFD constant. At maximum value of grit size(450µm), %∇Ra decreases with an increase in diamond percentage in magnetic abrasives, but, at minimum grit size (60µm) , variation in %∇Ra is negligible as diamond percentage increases from 5% to 25%.

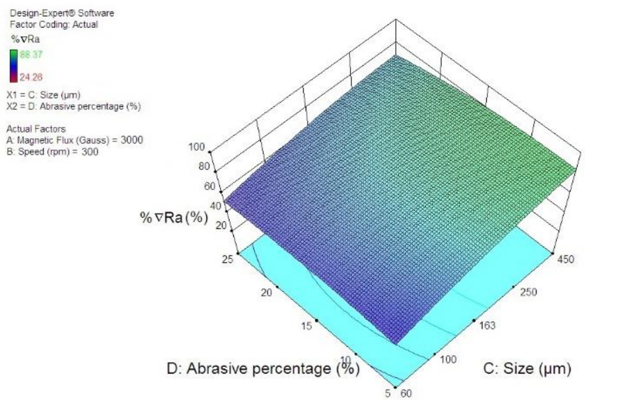

Fig. 8. Interaction effects of Grit Size (C) and %age of the abrasive (D) on the %∇Ra

%∇Ra increases with an increase in grit size of magnetic abrasives at a particular percentage of diamond in magnetic abrasives. It is seen that maximum %∇Ra is obtained at a lower percentage of abrasive (5%) and a maximum value of grit size of magnetic abrasive (450 µm). It is due to the fact that with a larger abrasive size, more abrasion takes place, resulting in a higher value of %∇Ra.

4. MICROSCOPIC AND SURFACE PROFILE EXAMINATION

In order to provide a more detailed analysis of the surfaces generated by the magnetic abrasive finishing experimentation, scanning electron micrographs (Figure 9) were taken before (a) and after (b) experimentation. Observation reveals that magnetic abrasive finishing successfully removed scratches and grinding marks. In order to continue to study the changes in the surface texture of the workpiece, the surface profile results before (a) and after (b) the MAF tests have been taken and are shown in Figure 10. A previously ground surface initially exhibits periodic peaks and valleys, but after finishing, the peaks were sheared down to a much smaller height, resulting in a smoother surface profile.

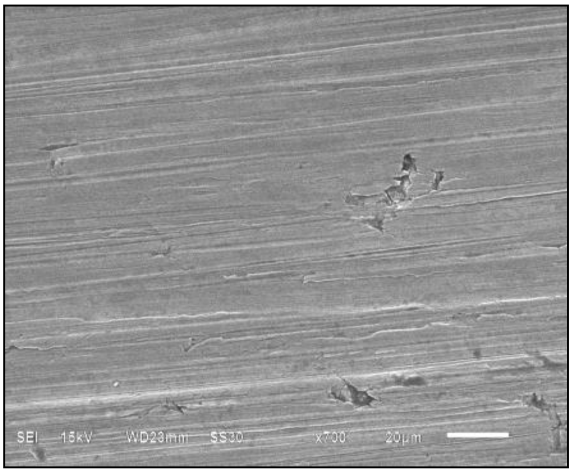

Fig. 9(a). SEM images of the surface before MAF

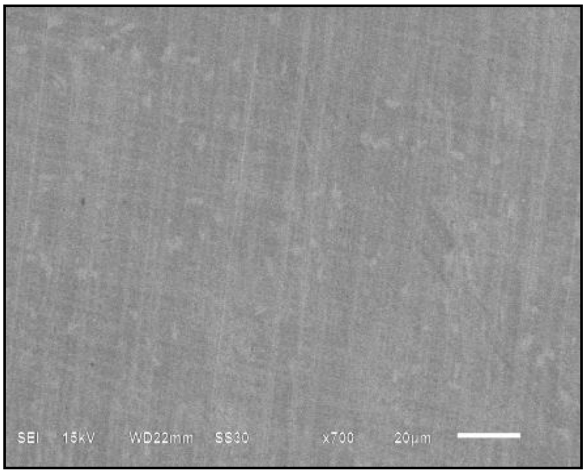

Fig. 9(b). SEM images of the surface after MAF

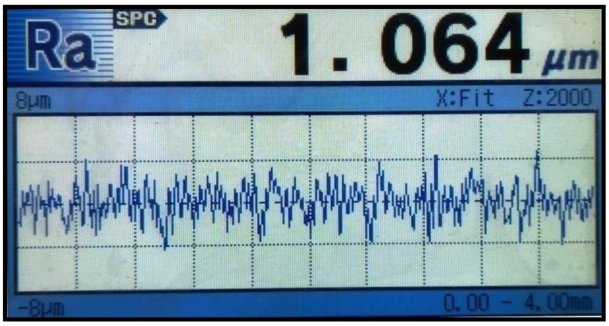

Fig. 10(a). Surface tester result of the surface before MAF

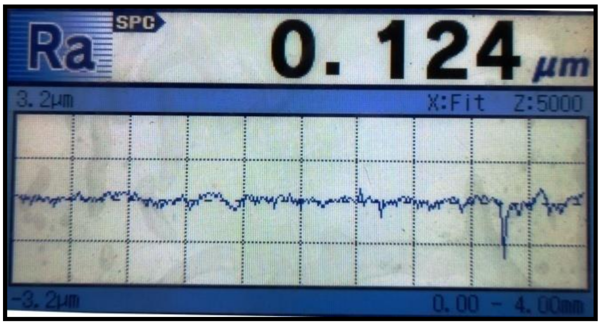

Fig. 10(b). Surface tester result of the surface after MAF

5. CONCLUSIONS

In this study response surface methodology was applied to develop a model and to optimize the process parameters. The process yields best results when magnetic flux density (A) = 3100 Gauss, rotational speed of poles (B) = 250rpm, grit size (C) = 250µm and percentage of abrasive particles (D) =10% for a percentage reduction in surface roughness. The maximum value of percentage reduction in surface roughness (%∇Ra) obtained in this work is 88.37%. Among the four factors, the grit size of the abrasives is the factor with the highest contribution (42.70%) and the rotation speed of the magnetic pole is the factor with the least contribution (0.79%) during the finishing process of the magnetic abrasive, which affects the percentage reduction in surface roughness (%Ra). In addition to grit size of abrasives, magnetic flux density significantly affected percentage reduction in surface roughness (%∇Ra). A higher value of magnetic flux and a larger grit size of abrasive are effective for getting a finer surface. As compared to the low rotational speed of the pole (200 rpm), better %∇Ra is obtained at a higher rotational speed of the poles (440 rpm). The intermediate value of the percentage of abrasive particles (15%) is found to be more effective in getting better %∇Ra than the lower (5%) and higher (25%) values of the percentage of abrasive particles. Based on the profiles and micro images of polished surfaces, it can be stated that this alternative approach of magnetic abrasive finishing is equally an effective method for finishing stainless steel SS304 sheets.

6. REFERENCES

1. Shinmura, Takeo, KoyaTakazawa, EijiHatano, and Toshio Aizawa. (1984)*"Study on Magnetic Abrasive Process- Finishing Characteristics."* Bull. Japan Society of Precision Engineering 18.4, pp. 347-48.

2. Jain, V., Kumar, P., Behera, P., &Jayswal, S. (2001) *"Effect of working gap and circumferential speed on the performance of magnetic abrasive finishing process."* Wear, **250**(1-12), pp. 384-390.

3. Singh, Dhirendra K., V.k. Jain, and V. Raghuram.

"Parametric study of magnetic abrasive finishing process." Journal of Materials Processing Technology 149.**1-3** (2004): 22-29.
4. Singh*, D. K., Jain, V. K., & Raghuram, V. (2005) *"On The Performance Analysis Of Flexible Magnetic Abrasive Brush"* Machining Science and Technology, **9**(4), 601-619.
5. Girma, B., Joshi, S. S., Raghuram, M. G., & Balasubramaniam, R. (2006) "*AN EXPERIMENTAL ANALYSIS OF MAGNETIC ABRASIVE FINISHING OF PLANE SURFACES"* Machining Science and Technology, **10**(3), 323-340.
6. Mulik, Rahul S., and Pulak M. Pandey. (2010) *"Magnetic abrasive finishing of hardened AISI 52100 steel"* The International Journal of Advanced Manufacturing Technology, **55**(5-8), pp. 501–515.
7. Riveros, Raul E., Hann, Jared N., Taylor, Curtis R., Yamaguchi, H. (2013) "*Nanoscale Surface Modifications by Magnetic Field-Assisted Finishing."* Journal of Manufacturing Science and Engineering, **135**(5), pp. 051014-1-7.
8. Verma, Girish Chandra., Kala, Parteek., Pandey, Pulik Mohan.,. (2016) *"Experimental investigations into internal magnetic abrasive finishing of pipes."* The International Journal of Advanced Manufacturing Technology, **88**(5-8), pp. 1657–1668.
9. Jain V, Saren K, Raghuram V, Sankar M. (2016) *"Force analysis of magnetic abrasive nano-finishing of magnetic and non-magnetic materials."* The International Journal of Advanced Manufacturing Technology, **100**(5-8), pp.1137-1147.
10. Amnieh, SasanKhalaj, Mosaddegh, P., Tehrani, A.F., (2017) *"Study on magnetic abrasive finishing of spiral grooves inside of aluminum cylinders."* The International Journal of Advanced Manufacturing Technology, **91**(5-8), pp. 2885–2894.
11. Kajal, S., Jain, V. K., Ramkumar, J., &Nagdeve, L. (2017) *"Experimental and theoretical investigations into internal magnetic abrasive finishing of a revolver barrel."* The International Journal of Advanced Manufacturing Technology. **100**(5-8), pp. 1105–1122.
12. Wang, R., Lim, P., & Mun, S. D., (2017) *"Magnetic Abrasive Finishing for Inner surface of Al 6063 pipe: Experimental Investigations."* International Journal of Current Engineering and Technology. **7**(3), pp. 1178–1185.
13. Kumar V, Sharma R, Dhakar K, Singla Y, Verma K., (2019) *"Experimental evaluation of magnetic abrasive finishing process with diamond abrasive."* International Journal of Materials and Product Technology. **58**(1):55.
14. Yin C, Wang R, Kim J, Lee S, Mun S., (2019) *"Ultra-High-Speed Magnetic Abrasive Surface Micro-Machining of AISI 304 Cylindrical Bar."* Metals. **9**(5):489.
15. Xie, H., Zou, Y., Dong, C., & Wu, J., (2019) *"Study on the magnetic abrasive finishing process using alternating magnetic field: Investigation of mechanism and applied to aluminum alloy plate."* The International Journal of Advanced Manufacturing Technology. **102**(5-8), pp. 1509–1520.
16. Li, W., Chen, Y., Cheng, M., &Lv, Y., (2020) *"Effect of magnetic head shape on processing of titanium Alloy wire by Magnetic Abrasive Finishing."* Materials.**13**(6), 1401.
17. Nam S, Kim J, Mun S., (2020*) "Magnetic Abrasive Finishing of Beta-Titanium Wire Using Multiple Transfer Movement Method."* Applied Sciences. **10**(19):6729.
18. Zhang, Y., & Zou, Y., (2021) *"Study of corrective abrasive finishing for plane surfaces using magnetic abrasive finishing processes."* Nanotechnology and Precision Engineering. **4**(3), 033001.
19. Lee P, Chang J., (2021) *"A magnetic abrasive finishing (MAF) platform utilizing horizontal transverse magnetic field magnetized by permanent magnets."* Microsystem Technologies. **27**(6), pp.2499-2506.
20. Xie H, Zou Y., (2021) *"Study on the magnetic abrasive finishing process using alternating magnetic field—discussion on the influence of current waveform variation."* The International Journal of Advanced Manufacturing Technology. 2021, **114**(7-8), pp. 2471-2483.
21. Ahmadi F, Beiramlou H, Yazdi P., (2021) *"Effect of abrasive particle morphology along with other influencing parameters in magnetic abrasive finishing process."* Mechanics & Industry. 22:15.

7. ACKNOWLEDGEMENTS

The authors thank the Department of Mechanical Engineering, I.K. Gujral Punjab Technical University, Kapurthala, India, for their support.

Received: March 06, 2022 / Accepted: June 15, 2022 / Paper available online: June 20, 2022 © International Journal of Modern Manufacturing Technologies